State of Wisconsin
Department of Administration
Division of Energy

Environmental Research Program

Final Report

August 2005

Toxicity of Secondary Coal Combustion Emissions in Wisconsin

Prepared by:
Dr. Annette Rohr, Electric Power Research Institute (EPRI)
Dr. Petros Koutrakis, Harvard School of Public Health
Dr. John Godleski, Harvard Medical School and Harvard School of Public Health

This report in whole is the property of the State of Wisconsin, Department of Administration, Division of Energy, and was funded through the FOCUS ON ENERGY program.

EXECUTIVE SUMMARY

Date of Report: July 15, 2005

Title: Comparative Toxicity of Secondary Coal Combustion and Mobile Source Emissions in Wisconsin

Investigators: Dr. Annette Rohr, Project Manager, Air Quality, Health and Risk, Electric Power Research Institute (EPRI)
Dr. Petros Koutrakis, Professor, Harvard School of Public Health
Dr. John Godleski, Associate Professor, Harvard Medical School and Harvard School of Public Health

Institutions: Electric Power Research Institute, Harvard School of Public Health

Research Category: Program Interest Area A: Effect of air pollutants from coal-fired power plants on human health in Wisconsin

Project Period: September 1, 2002 – June 30, 2005

Objectives of Research: Much of the research on the health effects of power plant emissions has used coal fly ash or a pilot combustor, neither of which accurately reflects exposure to the secondary particulate matter (PM) formed through atmospheric oxidation of power plant emissions. This project involves exposing laboratory rats via inhalation to realistic coal-fired power plant and mobile source emissions to help determine the relative toxicity of these PM sources. The emissions are then extensively characterized to provide insight into the gas- and particle-phase components contributing to toxicity. Multiple pulmonary and cardiovascular toxicological endpoints are evaluated. In addition to normal, a model of susceptibility (the myocardial infarction [MI] model) was proposed in light of the cardiovascular effects of PM. Thus, the primary objective of the project is to increase understanding of the PM sources and components responsible for adverse health effects, specifically as these relate to coal combustion and mobile source emissions. A secondary objective is to provide insight into atmospheric conditions most likely to result in the formation of products which could lead to health effects, through the simulation of multiple atmospheric conditions.

Summary of Research/Accomplishments: This project was technically challenging by virtue of its novel design and requirement for the development of new techniques. Previous studies have either involved instillation of collected coal fly ash, or have carried out inhalation exposures to emissions from lab-scale combustors. Neither of these approaches accurately simulates population exposures to atmospheric PM derived from coal combustion, largely because with the widespread introduction of particulate controls on power plants, primary PM emissions are very low. It is the secondary particulate matter formed from SO_2 and NO_x in stack emissions as well as any residual primary PM that is of interest. No efforts to consider and account for secondary atmospheric chemistry have been made to date. By examining aged, atmospherically transformed aerosol derived from stack emissions, the subject project has been able to evaluate the toxicity of coal combustion emissions in a manner that more accurately reflects the exposure of concern.

The subject study also involved assessment of actual plant emissions in a field setting – an important strength since it reduces the question of representativeness of emissions.

Initially, a sampling system consisting of a venturi orifice and aspirator was assembled to draw emissions from the stack. However, after testing the equipment at the plant, it was suspected that primary particle losses may have been occurring in the sampler, and the sampling system was redesigned. The modified system resulted in no substantial increase in particle concentration in the emissions. This observation, coupled with stack sampling conducted according to standard EPA protocol, led us to the conclusion that the sampled emissions are representative of those exiting the stack into the atmosphere.

Two mobile laboratories were outfitted for the study: (1) chemical laboratory in which the atmospheric aging was conducted and which housed the bulk of the analytical equipment; and (2) toxicological laboratory, which contained animal caging and the exposure apparatus.

Animal exposures began in May 2004, and were carried out as follows:

- May 10-13, 2004: primary emissions
- June 22, 23, 25, and 26, 2004: oxidized, neutralized emissions + secondary organic aerosol (SOA)
- June 27-30, 2004: oxidized, neutralized emissions + SOA
- October 4-7, 2004: oxidized emissions (unneutralized) + SOA
- October 11-14, 2004: oxidized, neutralized emissions + SOA
- November 13-15, 2004: oxidized emissions (unneutralized)

Toxicological endpoints included (1) pulmonary function and breathing pattern; (2) bronchoalveolar lavage fluid cytological and biochemical analyses; (3) blood cytological analyses; (4) *in vivo* oxidative stress in heart and lung tissue; and (5) heart and lung histopathology.

Results indicated no differences between exposed and control animals in any of the endpoints examined. Exposure concentrations for the scenarios utilizing secondary particles (oxidized emissions) ranged from 70 - 256 $\mu g/m^3$, and some of the atmospheres contained high acidity levels (up to 49 $\mu g/m^3$ equivalent of sulfuric acid). However, caution must be used in generalizing these results to other power plants utilizing different coal types and with different plant configurations, as the emissions may vary based on these factors.

Future Directions/Activities: This project is part of a larger research effort, the TERESA (Toxicological Evaluation of Realistic Emissions of Source Aerosols) Study. TERESA includes fieldwork and assessment of health effects at three power plants: (1) the subject plant in this report, located in Wisconsin and burning Powder River Basin coal; (2) a plant in the Southeast burning low-to-medium sulfur eastern bituminous coal; and (3) a plant in the Midwest burning medium-to-high eastern sulfur bituminous coal, with a scrubber. Work at these latter two plants is being partially funded by the U.S. Department of Energy's National Energy Technology Laboratory (DOE-NETL). For additional information on this larger study, please visit http://www.netl.doe.gov/coal/E&WR/air_q/index.html.

The subject project also includes assessment of the toxicity of mobile source emissions, being funded from other sources. However, we have not yet conducted these experiments due to the mobile laboratories being occupied with the coal combustion emissions work. The mobile source work will be conducted at the conclusion of the TERESA program, after the three plants have been investigated, and the findings will be reported in an addendum to this report.

TABLE OF CONTENTS

LIST OF FIGURES

LIST OF TABLES

1.0 INTRODUCTION

In the face of further regulation of particulate matter (PM), there is a critical need for increased knowledge regarding the PM sources and components responsible for the health effects observed in epidemiological and toxicological studies. Currently, PM is regulated as if it and its constituents were toxicologically identical, regardless of contributing sources, using a mass-based standard. Recent findings from a large epidemiological study in Atlanta, GA (ARIES) point to the importance of the carbon-containing fraction of PM, which may be derived from mobile, biogenic, and other sources (e.g., fireplaces, agricultural burning) (Klemm et al., 2005; Metzger et al., 2004; Peel et al., 2005; Sinclair and Tolsma, 2005).

The project reported on here investigates the role played by specific emissions sources and components in the induction of adverse health effects by examining the relative toxicity of coal combustion and mobile source (gasoline and/or diesel engine) emissions and their oxidized products. The work is a significant improvement over previous studies to investigate the toxicity of coal combustion-derived particulate matter by virtue of several highly innovative and unique design features. First, all toxicological studies of coal combustion emissions to date (some of which have shown biological effects) have used primary PM, ie. coal fly ash (e.g. MacFarland et al., 1971; Alarie et al., 1975; Raabe et al., 1982; Schreider et al., 1985). The relevance of primary PM to human population exposure is unclear, since emissions of primary PM are now very low with the widespread introduction of particulate controls on power plants. It is the secondary particulate matter formed from SO_2 and NO_x in stack emissions as well as any residual primary PM that is of interest. No efforts to consider and account for secondary atmospheric chemistry have been made to date. By examining aged, atmospherically transformed aerosol derived from stack emissions, the subject project has been able to determine the toxicity of emissions sources in a manner that more accurately reflects the exposure of concern. In addition, the atmospheric simulation component of the project allows the investigation of the effect of different atmospheric conditions on the formation and toxicity of secondary PM. Second, the primary PM used in the studies to date has typically been generated through the use of pilot combustors in a laboratory setting. There is concern that pilot combustors may not accurately mimic stack emissions due to differences in surface to volume ratios and thus time-temperature histories. The subject study involved assessment of actual plant emissions in a field setting – an important strength of the study since it eliminates any question of representativeness of emissions.

The study involves on-site sampling and dilution of coal combustion emissions at three coal-fired power plants, as well as mobile source emissions. Emissions are introduced into a reaction chamber that simulates oxidative atmospheric chemistry, and both primary and secondary materials are extensively characterized, including NO_2, SO_2, ozone, NH_3, hydrocarbons, particle number and mass (including ultrafines), sulfate, nitrate, elemental/organic carbon (EC/OC), ammonium, and metals. Test atmospheres containing diluted emissions and oxidized emission products are utilized in two toxicological assessment steps, the first utilizing normal laboratory rats, and the second consisting of a comprehensive toxicological evaluation in a rat model of susceptible individuals. This last step includes telemetric methods for the assessment of cardiac function.

The primary objective of the project is to evaluate the potential for adverse health effects from ambient exposure to realistic coal-fired power plant emissions. Secondary objectives of the study are to: (1) evaluate the relative toxicity of coal combustion emissions and mobile source emissions, their secondary products, and ambient particles; (2) provide insight into the effects of

atmospheric conditions on the formation and toxicity of secondary particles from coal combustion and mobile source emissions through the simulation of multiple atmospheric conditions; (3) provide information on the impact of coal type and pollution control technologies on emissions toxicity; and (4) provide insight into toxicological mechanisms of PM-induced effects, particularly as they relate to susceptible subpopulations.

2.0 EXPERIMENTAL

2.1 Emissions Sampling System

The emissions sampling system is described in detail in a manuscript currently in preparation (Ruiz et al., 2005a). The initial design and final modifications of the emissions sampling system represented a technical challenge, with significant care being taken to avoid particle losses in the system. A continuous sample passed through a stainless steel tube running from the pre-stack duct to a mobile chemical laboratory on the ground. The sampling tube had a size selective inlet to remove particles nominally larger than 2.5 μm and ports for the addition of filtered (dry) air. Dilution air cooled the exhaust to normal ambient temperature and dried the exhaust to prevent condensation of water in the sampling line. It also reduced gas concentrations to appropriate levels for the reaction chamber and to result in target secondary particle concentrations of 200-300μg/m^3. Sampling flow rate, dilution airflow, and tubing dimensions were optimized to minimize losses of ultrafine particles, SO_2, and acidic sulfate particles.

During initial testing at the plant in May, low and highly variable particle number and mass concentrations were measured in the primary emissions. Primary PM concentrations during the first animal exposures in May ranged from 0.5 –1 μg/m^3, and particle counts were approximately 1000 cm^{-3}. We speculated that the original sampling system (venturi aspirator and orifice) may have produced a sampling artifact by artificially increasing particle losses, and a new sampling system was designed. This system operated on the simple principle of flow balance. A pulling pump was placed at ground level, drawing approximately 202 LPM, while a clean air flow of 200 LPM was adjusted at the sampling port. A Tee fitting connecting the clean air flow, the sampling port, and the transmission tubing connected to the pump at ground level was installed, allowing a stack sample to be automatically collected and diluted. A valve at ground level allowed control of the amount of flow pulled by the pump, thereby controlling the dilution ratio. Surprisingly, results from this system did not show any improvement over the previous sampling system. On the contrary, this system raised issues related to flow control and dilution ratios. In addition, it created a large pressure drop in the chemical laboratory that was not suitable for the particle measurement instruments. It was therefore concluded that this system was not suitable for use.

Further investigation of the sampling port using the aspirator and critical orifice technique was then carried out. The temperature in the sampling tube connecting the interior of the stack to the aspirator was found to be extremely important. Using thermocouples, the temperature in the tube was measured. Using the past configuration used for the previous animal exposures (in May), the temperature in the tube was found to be about 60 C. Under these conditions, there was large variability in particle size distribution. The most uncertain element was a mode of small particles ranging from 10 to 50 nm, which changed dramatically during the day with respect to particle number, size distribution, and mass. In contrast, when the tube temperature was adjusted to an optimal 100 C, the emissions stabilized in a constant and repeatable size distribution. Particle number appeared to be lower, but particles were larger, centered around 100 to 150 nm.

We believe that this is representative of the true emissions, and that the particles observed at non-optimal temperature represent particle condensation occurring in the sample tube. We believe that it is the sulfur trioxide gas (SO_3) present in the emissions that reacts with water to form new H_2SO_4 particles.

A modification of the sampling system was then tested. In this test the critical orifice was replaced by a stainless steel tube of about 1 meter long and 0.12" ID. This tube restricted the flow and thus controlled the sample flow. The dilution ratio was easily controlled by changing the pressure drop applied at ground level. This system allowed testing of different dilution ratios.

Using this technique, we determined whether changing the flow through the sampling tube affected the quality of the aerosol sampled. It was hypothesized that if there were any loss mechanism in the tube, the losses should be decreased if the residence time is decreased in the tube. This proved not to be the case for small particles. Measurements made with the SMPS showed that the size distribution was not changed by changing dilution ratio (residence time in the tube). Total particle counts were also unchanged, with particle concentration corrected for dilution and representing in-stack concentrations. For larger particles measured using the APS, a lower dilution ratio was found to improve particle collection. This may be the effect of the residence time, but we also believe that it may be the effect of removing the back pressure at ground level, which improves the particle collection efficiency for big particles. The final dilution sampling scheme employed is shown in Figure 1. Note that this scheme was used for exposure Rounds 4-6, while the orifice/cyclone system was used for Rounds 1-3 (details of exposure rounds are provided in Section 3.0, Table 1).

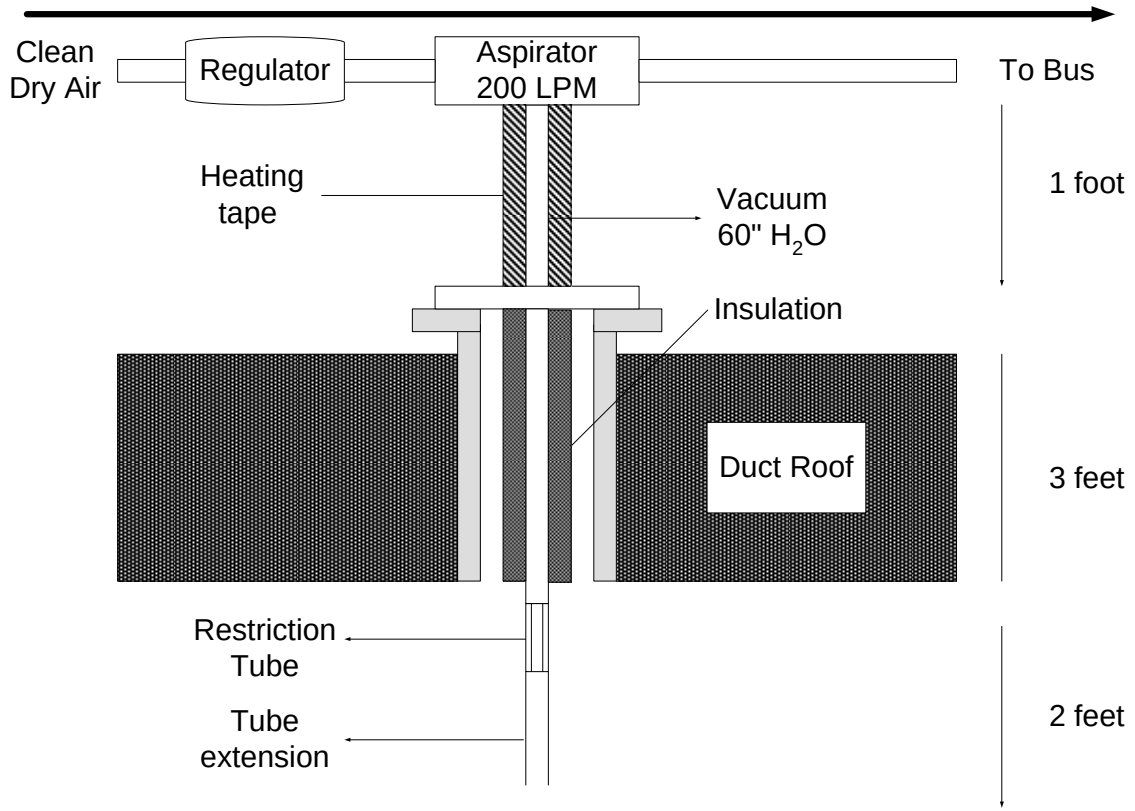

Figure 1. Final configuration of emissions sampling system.

2.2 Atmospheric Reaction Simulation System

The atmospheric reaction simulation system is described in detail in a manuscript currently in preparation (Ruiz et al., 2005b). The system consists of dual chambers (Figure 2). This dual-chamber conceptual model and physical configuration assumes that the oxidation of SO_2 to form H_2SO_4 takes place primarily in the plume that is formed from the initial dispersion of the emitted stack gas. In the first chamber, SO_2 reacts with hydroxyl radicals -- produced from the reaction of water vapor with $O(^1D)$ from the photolysis of ozone by UV light -- to form H_2SO_4. Relatively high intensity UV light was used to produce sufficient hydroxyl radical concentrations to oxidize the SO_2. The second stage occurs when the H_2SO_4 mixes with and is neutralized by ammonia introduced to the chamber to simulate that from ground level sources, and where the neutralized or acidic sulfate particles also mix, independently, with introduced VOCs to simulate those from both anthropogenic and natural sources, and particle-phase organics are formed. Thus, in the TERESA system, in the second reaction chamber, the acidic aerosol can be neutralized with ammonia, and/or α-pinene (as a representative biogenic VOC) can be reacted with ozone to produce organic particulate matter, depending on the scenario desired.

Reaction Chambers

The first stage reaction chamber is 152 x 122 x 30 cm, with a total volume of approximately 500L. The side (152 x 30 cm) and end (122 x 30 cm) surfaces of the chamber are made of opaque PTFE Teflon sheet. The larger 152 x 122 cm top and bottom surfaces are made of transparent PTFE Teflon film (in order to transmit UV irradiation). The chamber was designed to attach and detach the Teflon film easily, allowing periodic sheet replacement. Also, the chamber has wheels that facilitate its movement into and out of an enclosure that holds an array of UV lamps that face the two transparent Teflon film surfaces of the chamber.

The second stage reaction chamber has glass walls coated with Teflon lubricant to minimize wall reactions. The dimensions are 60 x 50 x 30 cm with a total volume of 90 L. At 5 LPM the residence time in the chamber is 18 minutes. A schematic of the dual chamber reaction scheme is shown in Figure 2.

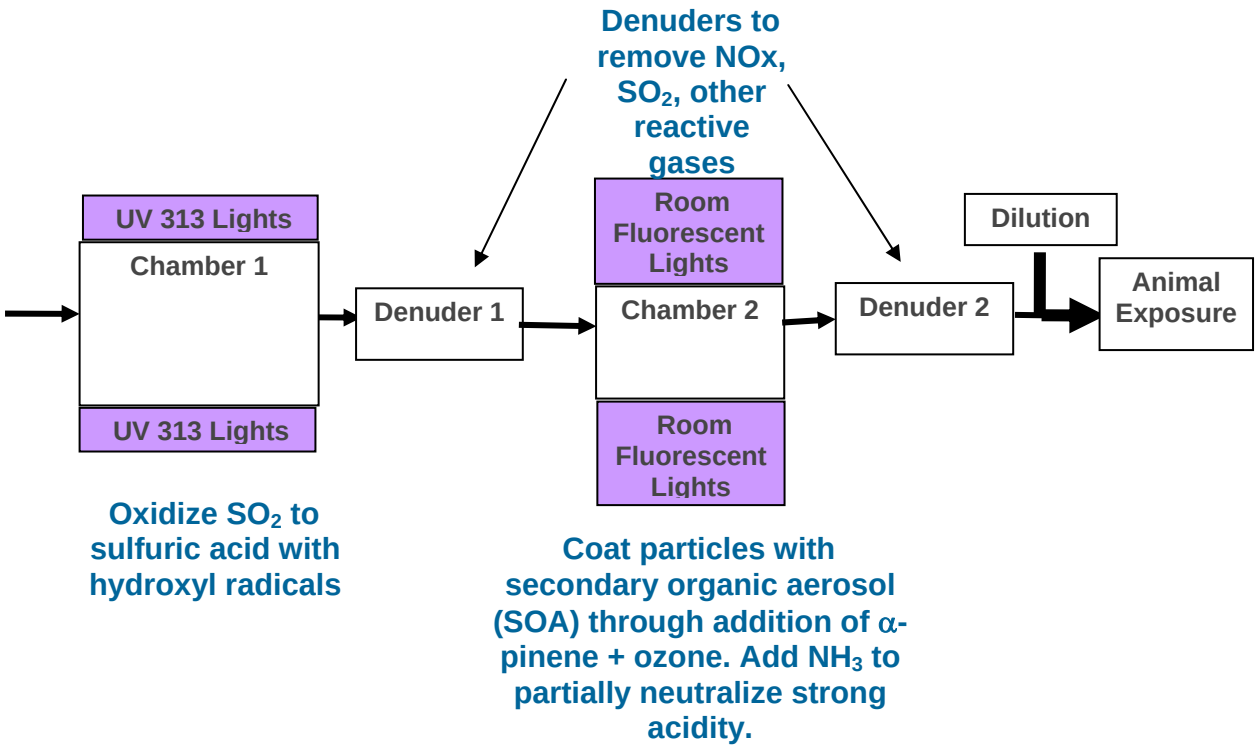

Figure 2. Dual chamber system for atmospheric simulations.

Banks of lamps are present on the sides of Chamber 1, about 10 cm from the Teflon film walls. The chamber and lamps are enclosed in an opaque box that protects personnel from UV light exposure and uses ventilation to remove excess heat and thus control chamber temperature when lamps are on. As light sources we used UVB-313 lamps (Q-Panel Lab Products, Cleveland, OH) with a 0.127 mm Cellulose Acetate film (CA, supplied by McMaster-Carr, New Brunswick, NJ) used as a light filter for wavelengths below 295 nm (McLeod, 1997; Holmes, 2002). Wavelengths below 295nm are not present in the ground level solar spectra and therefore these wavelengths were removed to ensure that they did not catalyze any type of reaction that we were not aware of and that does not occur in the troposphere.

A spectroradiometer with a light integration head (Model SPEC UV/PAR, Apogee Instruments Inc., Logan, UT) was used to characterize the light spectrum of the lamps alone and with CA. All the spectra were acquired with the integrating head placed 10 cm directly above and 30 cm from the end of a 2-lamp T12 fixture. For these tests, the pilot chamber was used and irradiated with UVB-313 lamps covered with CA film. Figure 3 shows that CA effectively filters light below 295 nm while it transmits lights above 300 nm.

.

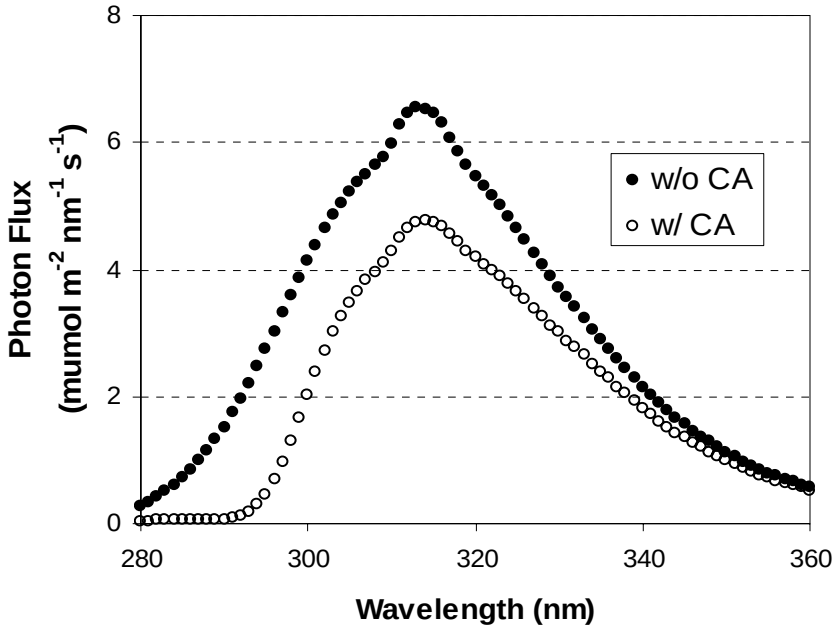

Figure 3. Characteristics of light sources: Light spectra of UVB313 lamps alone and covered with CA film.

Removal of Excess Reactive Gases

Excess reactive gases are removed from the first stage reaction mixture (while keeping the secondary particles suspended in air) using denuders. The denuder system is described in detail in Ruiz et al. (2005c). The reaction mixture that is drawn out of the first chamber passes through a counter-current diffusion denuder that removes 80-90% of the SO_2, NOx, and ozone. A second denuder system is employed downstream of the second chamber to remove excess gas-phase organics and ozone, as well as to further reduce SO_2 and NOx concentrations prior to animal exposures.

The first denuder operates by drawing the mixture of secondary particles and reactive gases through an inner channel. Clean air is passed in a counter-flow fashion through two outer channels. Microporous PTFE Teflon membranes are placed between the inner and outer channels. Gaseous species diffuse through the membranes from the inner to the outer channels, while particles pass through the denuder. An empirical model was derived, and performance was evaluated with CO, SO_2, and SF_6 (which represent molecules with very different diffusion coefficients). Residual values (fraction of the gas that passes through the denuder and does not penetrate through the membrane) for various testing conditions were determined. Results show that the residual value for SO_2 is 15% at a 2:2:1 (top outer:bottom outer:inner channels) flush ratio, while that for CO is 16% and 10% at flush ratios of 1:1:1 and 2:2:1, respectively, indicating that the denuder is performing as expected. Particle losses were characterized and found to be constant as a function of size in the ultrafine fraction (~20-30%), while lower for larger size fractions.

2.3 Exposure Measurements

Analytical measurement of the exposure atmospheres was extensive, and sampling was carried out at a number of locations in the chamber/denuder system (Figure 4). For the purposes of this report, the measurements at the animal exposure chambers are of greatest interest. At this sampling port, the following measurements were carried out:

Continuous Measurements

- $PM_{2.5}$ mass, using an R&P Tapered Element Oscillating Microbalance (TEOM)
- Particle number, using a condensation particle counter (CPC TSI 3022)
- SO_2 (pulsed fluorescence method)
- NO_x (chemiluminescence method)
- O_3 (UV absorbance method)
- Temperature
- Relative humidity (RH)

Integrated Measurements

- $PM_{2.5}$ mass (gravimetric analysis; Teflon filters)
- Particle sulfate (denuder/filter pack system, ion chromatography)
- Particle nitrate (denuder/filter pack system, ion chromatography)
- Particle strong acidity (denuder/filter pack system, pH Analysis)
- Particle ammonium (denuder/filter pack system, ion chromatography)
- Particle elements (X-ray fluorescence)
- EC/OC (thermal optical reflectance [TOR] method; quartz fiber filters)
- Sulfur dioxide (denuder/filter pack system, ion chromatography)
- Nitric acid vapor (denuder/filter pack system, ion chromatography)
- Nitrous acid vapor (denuder/filter pack system, ion chromatography)
- Ammonia (denuder/filter pack system, ion chromatography)
- Ketones and aldehydes (DNPH cartridges)
- α-pinene (Tenax tubes)

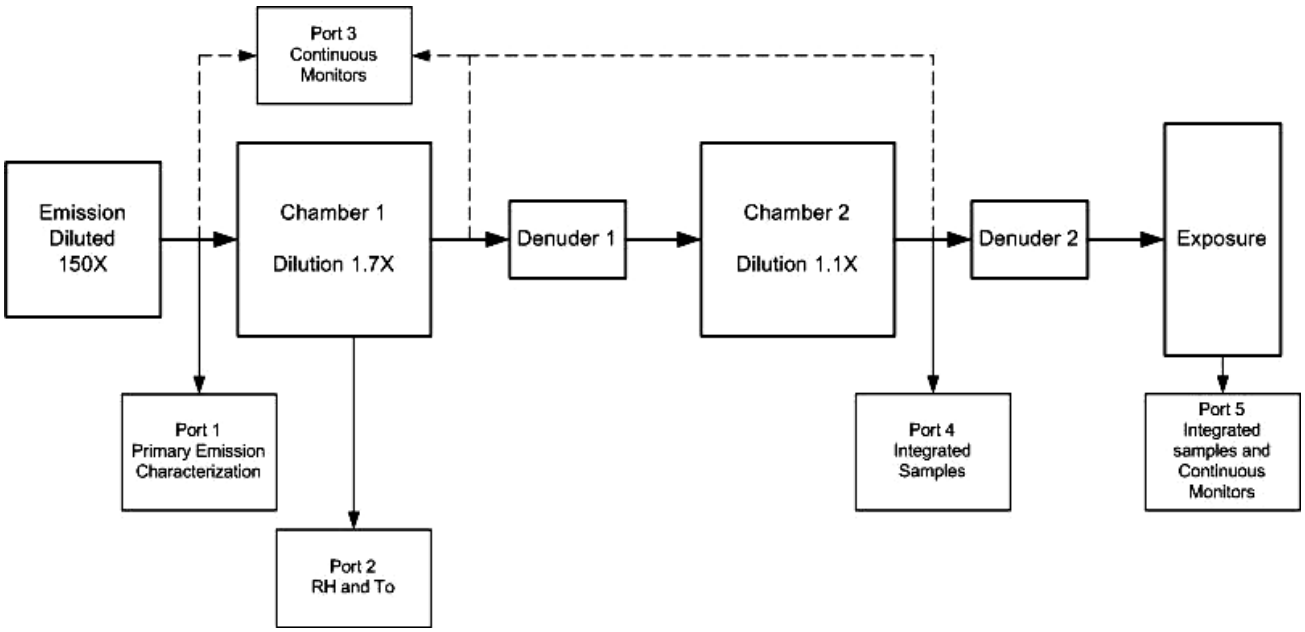

Figure 4. Location of sampling ports.

Originally, an aethalometer was to have been used to measure elemental/black carbon; however, because of the extremely low elemental carbon concentrations expected in the coal combustion emission scenarios, this was not employed. Similarly, CO monitoring, although originally proposed, was not carried out because it was expected to be extremely low after the dilution and denuder steps. Finally, the proposed elemental streaker was not used due to technical problems; however, elemental concentrations on 6-hour integrated samples were determined using XRF.

2.4 Animal Exposure Laboratory

From the reaction chamber, aged emissions enter a temperature- and humidity-controlled exposure chamber located in the mobile toxicological laboratory. This laboratory is comprised of a trailer outfitted with alarm systems and added electrical systems. Because a higher ventilation rate was needed, the trailer had to have a second electric service added to handle the larger heating requirement. This additional electrical capacity also provided more flexibility in the use of auxiliary equipment. The Harvard Animal Resource Committee (ARC) inspected the facility and approved it for use in field studies using animals.

2.5 Toxicological Methods

A two-stage toxicological assessment was proposed. In Stage I, overall cardiac and pulmonary toxicity would be determined in normal laboratory rats, followed by a more comprehensive and cardiac-focused Stage II assessment in a compromised rat model. However, because no adverse biological effects were observed in Stage I, the Stage II assessment was not conducted.

All exposures were carried out in female Sprague-Dawley rats. Each scenario included 4 days of exposures, each with 5 rats (2 for *in vivo* oxidative stress and 3 for the other biological

endpoints). Thus, for each scenario there were 6 rats in the oxidative stress group and 9 rats in which pulmonary function, BAL, and blood cytology are assessed. Animals were placed into modified whole-body plethysmographs during exposure. Exposures were 6 hours in duration. Animals were maintained and studied in accordance with the National Institutes of Health guidelines for the care and use of animals in research. All protocols were approved by the Harvard Medical Area Standing Committee on Animals.

In the Stage I toxicological assessment, pulmonary, cardiac, and systemic effects in normal rats were evaluated via bronchoalveoloar lavage (BAL), histopathology, pulmonary function, *in vivo* oxidative stress, and blood cytology.

Pulmonary Function and Breathing Pattern

Pulmonary function and breathing pattern were assessed using an automated software system (Buxco Biosystem 1.5.3A, Buxco Electronics, Sharon, CT), which calculates a number of respiratory parameters from flow changes in a pressure transducer connected to the plethysmograph. A rejection algorithm is automatically included in the breath-by-breath analysis. Markers of interest include peak expiratory flow (PEF), tidal volume (TV), respiratory frequency (*f*), and minute ventilation (MV).

Bronchoalveolar Lavage

BAL was performed through a tracheal incision using endotoxin-free Dulbecco's phosphate-buffered saline. The first lavage was 4 ml; subsequent lavages were ~5 ml, based on the body weight of the animals. Cell viability (> 95%) and total cell count were determined by hemacytometer counts of small aliquots of the re-suspended BAL fluid diluted in trypan blue solution. Cell type was determined from modified Wright-Giemsa-stained cytocentrifuge preparations; 200 cells were counted per sample. Within the acellular BAL supernatant, three markers of pulmonary injury were tested: (1) lactate dehydrogenase (LDH) as an indicator of cytotoxicity; (2) a lysosomal enzyme, β-n-acetyl glucosaminidase (βNAG), as a marker of phagocyte activation and lysing; and (3) total BAL protein as a marker of pulmonary inflammation and vasculature permeability. Total protein was measured using a standard kit from Pierce (Product #23235; Rockford, IL). Determination of βNAG and LDH were done by the methods of Selliger et al. (1960) and Pesce et al. (1964), respectively. Enzymatic reagents for the measurement of βNAG and LDH were obtained from Sigma Chemical Co (St Louis, MO) and chemical reagents were obtained from Fisher Scientific Co (Pittsburgh, PA). LDH measurements were performed using a Beckman DU-640 spectrophotometer (Beckman Instruments, Fullerton, CA) and βNAG was measured using a kinetic plate reader (Molecular Devices, Sunnyvale, CA). BAL fluid samples were frozen and stored for possible future analysis of cytokines or other inflammatory mediators.

Histopathology

At autopsy, lungs were fixed with 2.5% glutaraldehyde via the airways at 20 cm of H_2O. Total lung volumes were determined by displacement, and the lungs were cut horizontally into 2 mm numbered sections. Three 3 slices were randomly selected for processing by paraffin histology techniques.

In Vivo Oxidative Stress

Organ chemiluminescence (CL)) refers to the ultra-weak light emission produced by biological systems due to the de-excitation of high-energy by-products of the chain reaction of lipid peroxidation (Boveris and Cadenas, 1999; Boveris et al., 1980). Organ CL measures the steady-state concentration of singlet oxygen ($^1O_2$) and follows the square of the intracellular concentration of H_2O_2. The latter constitutes a unique experimental advantage of the technique, since small variations in H_2O_2 are exponentially reflected in the values of CL. Organ CL has been successfully used in models of oxidative injury in the intact lung (Gurgueira et al., 2002; Evelson et al., 2000; Turrens et al., 1988) as well as in the perfused lung *in vitro* (Barnard et al., 1993). Of particular relevance to this project, Gurgueira et al. used this method to assess heart and lung oxidative stress in rats after exposure to concentrated ambient particles (CAPs) and residual oil fly ash (ROFA).

After the exposure, the animal was anesthetized with pentobarbital (0.25mg/kg). A surgical procedure was performed to expose the heart and/or lungs to the counter of intrinsic chemiluminescence; the experimental setup is shown in Figure 5. In a dark field, the counter measured the chemiluminescence for 10 seconds, which was then sent to an amplifier to the computer, where the calculations were perfomed and expressed as counts per second per square centimeter (cps/cm^2). After the measurements, the animal was sacrificed by exsanguination, and the heart and the lungs were frozen for future TBARs analysis.

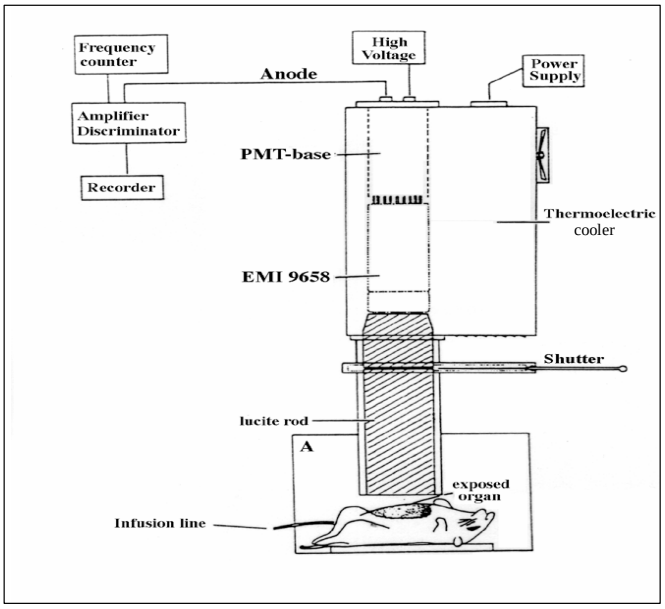

Figure 5. Single-photon counting apparatus used in chemiluminescence assay (from Boveris et al., 1980)

Blood Cytology

Blood cytology was evaluated 24 hours following the last day of exposure. Rats were euthanized with an overdose of sodium pentobarbital (65 mg i.p.). Blood was obtained by cardiac puncture. A 1 ml aliquot of whole blood was collected in a 1.5 ml EDTA-treated collection tube to prevent clotting. Total white blood cell counts (WBCC) and differential profiles were assessed at a commercial Veterinary Diagnostic Laboratory.

2.6 Statistical Analysis

For each biological endpoint, analysis of variance (ANOVA) tests were employed with SAS computer software to compare intra-animal alterations in physiological parameters due to exposure. Two-way ANOVA determinations were employed to determine if intra-group differences were significant. Differences are considered significant when $p < 0.05$.

3.0 RESULTS

Animal exposures were carried out between May and November, 2004, as summarized below in Table 1.

Table 1. Schedule of completion of fieldwork. Note that the neutralized secondary particle scenario with secondary organic aerosol was repeated 3 times.

Exposure Round	Scenario	Dates
1	Primary	May 10, 11, 12 and 13
2	Secondary + NH_3 + SOA (run 1)	June 22, 23, 25 and 26
3	Secondary + NH_3 + SOA (run 2)	June 27, 28, 29 and 30
4	Secondary + SOA	October 4, 5, 6 and 7
5	Secondary + NH_3 + SOA (run 3)	October 11, 12, 13 and 14
6	Secondary	November 13, 14 and 15

The Round 4 scenario (secondary particles + SOA) was originally not included in the study plan; however, we decided that this might be the most likely to induce biological effects, given that it would be highly acidic and contain SOA. Since we had not previously observed biological effects, it was deemed a useful scenario to investigate. We also repeated the most complex scenario (Round 2) since there had been a change in the sampling scheme from the June-July exposures. Round 6 was carried out with secondary aerosol and no additional components given that this material would also be highly acidic. We did not evaluate the neutralized, oxidized scenario because it is likely to be the least biologically potent scenario. Round 3 was carried out

during nighttime hours as it was believed that primary particles may be higher at that time due to changing plant load.

3.1 Stack Sampling Results

The objective of the stack sampling was to evaluate possible differences between in-stack primary $PM_{2.5}$ concentrations and the diluted concentrations used in the animal exposures. Low primary particle concentrations were found in the exposure scenarios conducted in May, based on the measurements of diluted samples determined by multiplying the measured concentrations in the diluted samples entering the reaction chamber by the dilution factor (about 150). Therefore, it was important to assess whether particle losses were occurring during dilution, and how the composition of the two types of samples (direct stack sampling and dilution sampling for animal exposures) might differ.

On October 19-21, 2004 in-stack sampling was carried out using a $PM_{2.5}$ cyclone with a filter holder placed inside the duct. Samples were collected on quartz fiber filters for periods of up to 4 hours (USEPA Conditional Test Method 040, December 3, 2002, *Method for the Determination of PM_{10} and $PM_{2.5}$ Emissions*, www.**epa**.gov/ttn/emc/ctm/ctm-**040**.pdf).

After the sampling had been carried out, it was determined that the in-stack sampling system had been operating with a lower cutpoint of approximately 1.9 µm because the flow measurement method that was tested in the laboratory did not work as expected for the field measurements. Consequently, the volumetric flow through the cyclone within the stack was actually higher than the target flow. The cutpoint was estimated using the simple theoretical principle that the cutpoint is proportional to the inverse square root of the ratio of the flows. It is also important to note that there was an evolution in the design of the sampling/dilution system. One early design used a cyclone (different from that used for the EPA in-stack method) but since we were not able to overcome the difficulties of using this cyclone (including the use of a venturi orifice to control the flow), we decided to use a sampling system that did not have an explicit size-selective feature. Consequently, it is possible that more particles larger than 1.9 µm were collected with the dilution sampling system than with the in-stack device. This would lead to higher mass values (after correcting for the dilution factor) for the dilution sampling system (assuming that losses of particles in this size region are negligible). In addition, a limitation of this type of testing is the fragility of the quartz filters. This led to high variability in the gravimetric blank samples, which prevented the accurate determination of mass concentration for the in-stack samples. Consequently, it is not possible to make a reasonable comparison of the mass concentration in-stack with the diluted sample measurements.

However, elemental (XRF) measurements are available that allow the comparison of composition of the in-stack and diluted samples. Because there was a large variation in the mass concentration for both the in-stack filter samples and the diluted filter samples, the best way to compare the composition is not the actual elemental concentrations in units of $\mu g/m^3$. Instead, we first estimate the total mass (TM) as represented by the sum of the mass contributions of the major oxides (MO) (based on the assumed most stable oxide for each major element) and the sum of the trace element mass concentrations (TE) (a very small fraction of the total):

$$TM = MO + TE \qquad \text{(Equation 1)}$$

Then, the mass fraction (MF) for each element is calculated using the mass concentration for each element (ME):

$$MF = ME/TM \quad \text{(Equation 2)}$$

For the comparison between the in-stack and diluted samples, the conventional "Enrichment Factor" (EF) is used. The concept of enrichment was developed to characterize the condensation of the most volatile elements that are in the vapor phase at the temperature of the stack gas, but condense to the particle phase when cooled and diluted. The EF for each element is calculated as follows:

$$EF = MF_{diluted}/MF_{in\text{-}stack} \quad \text{(Equation 3)}$$

The results of these calculations are shown in Figure 6. The estimated uncertainty values in the graph are shown with the hatched lines. Only values for element mass that were at least twice the XRF reported uncertainty for that element were used for these calculations. It is important to note that with relatively few values and substantial variations in the mass and elemental concentrations, these uncertainty values are only rough estimates of the true uncertainties. Nevertheless, the EF values for most elements are reasonably close to unity, suggesting that the composition of the particles was not changed substantially by dilution. The results for sulfur are particularly noteworthy because if there had been a considerable amount of vapor phase SO_3 in the hot stack gas, with the consequence that a substantial amount of this gas would condense as H_2SO_4 onto the cooled, diluted particles, then we would expect an EF value significantly higher than unity. So while we know that some SO_3 is added to improve the ESP efficiency, these results indicate that the amount remaining as vapor at the point of in-stack sampling is negligible (within the experimental error of our measurements) compared to the amount of particulate sulfur in the stack gas.

The EF values for Mn, Fe, and Zn (and perhaps Ba) indicate that there is relatively less of these elements in the diluted sample than in the stack gas. It is not difficult to provide a possible explanation for this result. As mentioned above, the 1.9 µm cutpoint of the cyclone for in-stack sampling is likely to be lower than the equivalent cutpoint of the dilution sampling system. If so, then relatively more of the larger particles will be collected using the dilution system. Since the composition of coal combustion particles is likely to vary with particle size, if there is relatively less of these four elements in the larger particles, their elemental MF values will be lower in the diluted samples than in the in-stack samples, and the EF values will be lower than unity, as observed. This explanation would also imply that for the other elements, there are negligible differences in composition for the different size fractions sampled by the two methods.

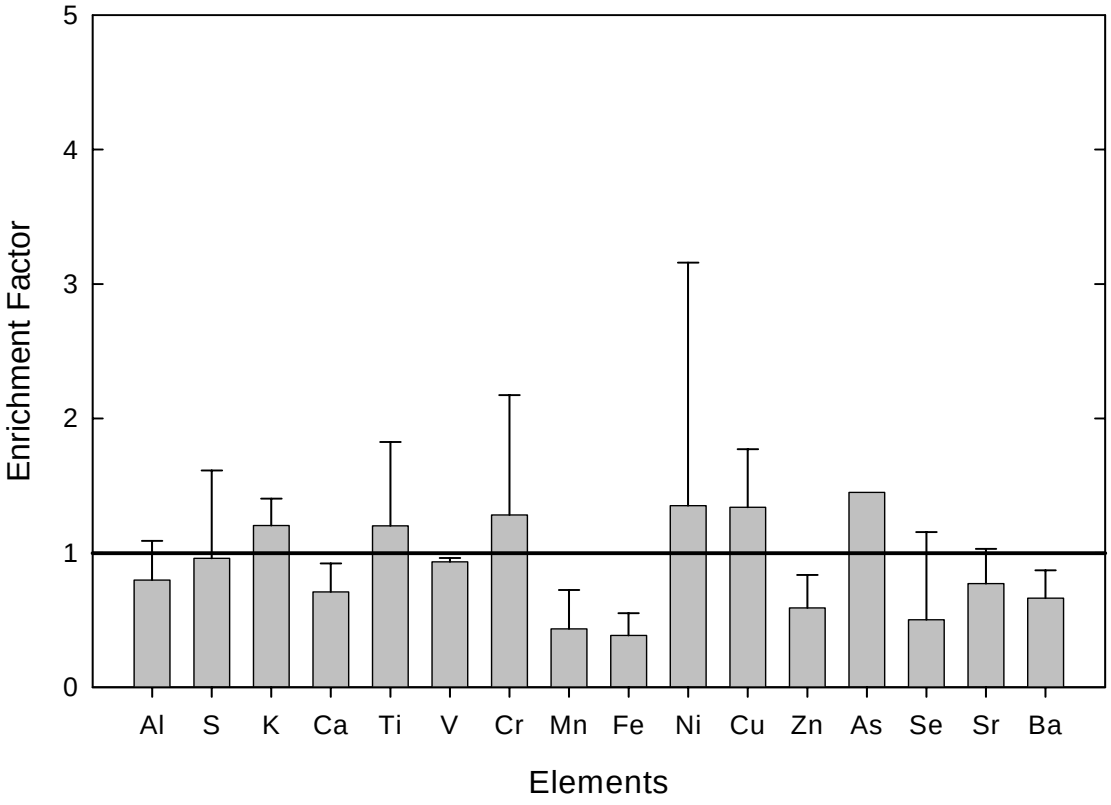

Figure 6. Enrichment Factors for elements between in-stack and diluted sample primary emissions.

No uncertainty value is shown for arsenic because there was only one XRF value each from all of the in-stack filters and from all of the diluted samples that was greater than twice the XRF reported uncertainty for this element. If we assume a similar uncertainty value for As to that of most of the other elements, it is unlikely that there is any difference between in-stack and diluted samples. However, if the EF value for arsenic is in fact significantly greater than unity, this would not be surprising because this element can have a significant fraction of its mass in vapor phase which could condense when it is cooled and diluted. However, selenium is another element that can behave similarly to arsenic, and it does not appear to show any significant enrichment.

An Estimated Mass concentration was based on the XRF elemental data using assumed major oxides plus trace elements. This value does not include silicon (since the filters are made of quartz fiber) and some ionic and carbonaceous species. For the in-stack samples, the estimated mass mean ± standard deviation value was 214 ± 41 $\mu g/m^3$, and the mean ratio of estimated to gravimetric mass was about 1.07, based on the single filter with a positive net mass before and after sampling. Taking into account the dilution factor of 150, the corresponding estimated mean concentration, based on the XRF elemental data for diluted samples (again using assumed major oxides plus trace elements) was 718 ± 410 $\mu g/m^3$. It is clear from these results that no significant

losses occur during the dilution sampling. Perhaps the reason why the dilution sample estimated mass results are higher than for the in-stack sampling is that many more particles larger than the 1.9 μm cutpoint of the in-stack sampling cyclone are collected by the dilution sampling system (that has no explicit size-selective feature).

3.2 Exposure Characterization Results

Summary results for PM-related measurements, gases, and elements are provided in Tables 2, 3, and 4, respectively, for all six experimental rounds.

Table 2. PM species concentrations, May-November, 2004. Mean and SD shown for each sampling round.

Exposure Parameter/Units	Concentrations					
	Round					
	1 Primary	2 Secondary + NH_3 + SOA	3 Secondary + NH_3 + SOA	4 Secondary + SOA	5 Secondary + NH_3 + SOA	6 Secondary
Mass [1] $\mu g/m^3$	2.3 ± 2.6	255.6 ± 27	241.1 ± 35.2	192.6 ± 73.3	141.2 ± 15.9	69.5 ± 10.4
Mass [2] $\mu g/m^3$	-0.2 ± 3.3	225.6 ± 42.1	178.5 ± 38.7	138.2 ± 53.4	116.8 ± 25.2	58.2 ± 5.8
GMD nm	380.3 ± 109.1	391.1 ± 14.5	389.4 ± 28.1	442.3 ± 37.5	373.1 ± 25.6	419.4 ± 45.7
Number Concentration $\#/cm^3$	1726 ± 1277	46892 ± 3905	42991 ± 2809	16924 ± 4495	66445 ± 8913	6723 ± 3550
Total Sulfate $\mu g/m^3$	0.7 ± 0.6	96 ± 18	76.9 ± 23.8	57.1 ± 24	38.7 ± 11	31.8 ± 1.3
Acid Sulfate $\mu g/m^3$	1.2 ± 0.2	27.3 ± 13.6	11.9 ± 7.7	49.1 ± 22.7	1.6 ± 1.7	22.5 ± 4
Nitrate $\mu g/m^3$	0.6 ± 0.5	24.9 ± 3.1	32.2 ± 8.6	1 ± 0.4	37.7 ± 6.2	1.1 ± 1.2
Ammonium $\mu g/m^3$	0.3 ± 0.3	25.8 ± 2.1	24.5 ± 5.6	3.1 ± 1.2	14.7 ± 4.1	3.3 ± 1.7
OC $\mu g/m^3$	24.6 ± 12.2	83.6 ± 24.4	62.9 ± 5.7	86.7 ± 7.1	57.6 ± 6.5	23.2 ± 7.4
EC $\mu g/m^3$	-1.4 ± 19.3	3.1 ± 38.6	3.8 ± 9	9.7 ± 11.2	1.9 ± 10.3	1 ± 11.6

[1] Continuous
[2] Integrated

Table 3. Gas concentrations, May-November, 2004. Mean and SD shown for each sampling round.

Compound	Concentrations					
	Round					
	1 Primary	2 Secondary + NH_3 + SOA	3 Secondary + NH_3 + SOA	4 Secondary + SOA	5 Secondary + NH_3 + SOA	6 Secondary
SO_2 (ppb) [1]	5.3 ± 4.4	11.5 ± 0.3	9.7 ± 4.1	17.5 ± 4.4	16 ± 3	9.3 ± 3.5
SO_2 (ppb)[2]	-[3]	31.5 ± 0.6	31.3 ± 5.9	38.9 ± 8.3	40.8 ± 3.8	31.7 ± 4.3
HNO_3 (ppb)	0.7 ± 0.4	2.6 ± 0.2	2.2 ± 0.4	1.6 ± 0.3	2.3 ± 0.7	0.6 ± 0.1
HONO (ppb)	2.7 ± 2.4	7.4 ± 1.6	9.8 ± 3.7	11.2 ± 5.1	7.8 ± 1.5	5 ± 1
NH_3(ppb)	26 ± 26.5	0.7 ± 0.2	0.8 ± 0.4	20.8 ± 3.8	16.1 ± 6.2	9.9 ± 6.2
NO(ppb)	5.9 ± 3.7	3 ± 1.2	3.6 ± 2.1	3.5 ± 2.9	4.6 ± 1.2	3.9 ± 0.5
NO_2(ppb)	6.7 ± 1.7	19.9 ± 2.2	20.8 ± 7.8	17.5 ± 6.6	10.1 ± 4.2	8.4 ± 1.8
O_3(ppb)	1 ± 1.2	34.9 ± 3.5	29.3 ± 2	26.8 ± 6.9	15.6 ± 6	26.9 ± 1
Formaldehyde (μg m^{-3})	-	24.9 ± 5.9	20.3 ± 4.1	16.1 ± 3.6	18.1 ± 3.9	-
Acetaldehyde(μg m^{-3})	-	6.4 ± 1.5	4.6 ± 0.2	5.2 ± 1	4.8 ± 0.6	-
Acetone (μg m^{-3})	-	16.6 ± 1.9	31.8 ± 16.2	15.5 ± 5.2	13 ± 2.9	-
Total carbonyls (μg m^{-3})	-	47.8 ± 7.7	56.7 ± 14.6	36.8 ± 9.2	35.9 ± 5.3	-
α-Pinene (μg m^{-3})	-	0.6 ± 0.1	1.2 ± 0.9	0.6 ± 0.1	0.8 ± 0.3	-

[1] Continuous
[2] Integrated
[3] Monitor not working

Table 4. Elemental concentrations, May-November, 2004. Concentrations for each exposure day and overall summary statistics. Values in bold represent significant measurements (measured value is more than 2 times its uncertainty).

		Concentrations (μg m^{-3})																						
Round	Day	Na	Mg	Al	Si	P	S	Cl	K	Ca	Ti	V	Cr	Mn	Fe	Ni	Cu	Zn	As	Se	Br	Pb	Sr	Ba	Cd
1	1	**0.503**	**0.142**	**0.070**	**0.093**	0.000	**0.064**	0.008	**0.017**	**0.097**	**0.013**	0.001	0.003	0.000	**0.057**	0.002	**0.005**	**0.006**	0.000	0.000	0.000	0.015	**0.007**	0.002	0.000
1	2	0.078	0.000	0.000	0.011	n/a	**0.043**	0.000	0.003	**0.034**	0.000	0.000	0.005	0.000	**0.024**	0.000	0.000	0.004	0.000	0.002	0.003	0.004	n/a	n/a	0.000
1	3	0.104	0.000	0.000	0.023	n/a	**0.024**	0.000	0.003	0.013	0.000	0.000	0.003	0.000	0.000	0.000	0.000	0.006	0.000	0.003	**0.007**	0.000	n/a	n/a	0.000
1	4	0.000	0.139	**0.063**	**0.095**	0.005	**0.086**	0.006	0.017	**0.049**	0.004	0.000	**0.008**	0.002	0.007	0.003	0.003	0.005	0.000	0.000	0.000	0.009	0.007	0.002	0.001
2	1	**0.661**	**0.178**	0.031	**0.058**	**n/a**	**43.220**	**0.301**	0.000	0.000	0.003	0.000	0.003	0.001	0.000	0.000	0.000	**0.006**	0.000	0.000	**0.015**	0.000	n/a	n/a	0.000
2	2	0.293	0.127	**0.069**	**0.074**	**n/a**	**27.860**	**0.280**	0.000	**0.072**	0.001	0.000	0.000	0.000	**0.022**	0.000	0.002	0.005	0.000	0.000	0.004	0.002	n/a	n/a	0.010
2	3	1.674	0.000	0.096	**0.399**	0.000	**37.308**	0.000	**0.029**	**0.084**	0.006	0.001	0.005	0.005	**0.035**	0.003	0.001	0.000	0.000	0.008	**0.017**	0.002	0.000	0.000	0.000
2	4	1.618	0.000	0.057	**0.432**	0.000	**34.876**	0.000	0.010	**0.022**	0.004	0.000	0.000	0.000	0.006	0.000	0.002	0.000	0.000	0.004	**0.012**	**0.029**	0.000	0.002	0.000
3	1	0.000	0.134	0.140	**0.439**	0.000	**36.030**	0.000	0.012	**0.030**	0.004	0.000	0.000	0.005	**0.014**	0.004	0.004	0.002	0.000	0.008	**0.010**	0.022	0.000	0.002	0.000
3	2	0.720	0.338	0.084	**0.236**	0.000	**32.111**	0.000	0.011	**0.015**	0.008	0.004	0.000	0.001	0.000	0.003	0.002	0.000	0.000	0.007	**0.017**	0.002	0.007	0.000	0.000
3	3	0.000	0.040	0.000	**0.027**	0.000	**19.245**	0.000	0.002	0.001	0.000	0.000	0.004	0.000	0.000	0.000	0.000	0.001	0.000	0.000	**0.011**	0.000	0.000	0.007	0.000
3	4	0.034	0.039	0.053	**0.043**	0.000	**33.286**	0.000	0.006	0.004	0.004	0.000	0.001	0.000	0.002	0.003	0.000	0.000	0.000	**0.009**	**0.020**	0.011	0.000	0.021	0.000
4	1	0.097	0.028	0.044	0.000	0.000	**25.256**	0.016	0.008	**0.038**	0.000	0.000	0.001	0.001	0.010	0.005	0.003	0.005	0.001	**0.014**	**0.029**	0.001	0.000	**0.045**	0.000
4	2	0.032	0.000	0.031	0.000	0.000	**16.839**	0.000	**0.030**	**0.038**	0.000	0.000	0.005	0.000	0.003	0.008	0.000	0.000	0.000	**0.013**	**0.018**	0.000	0.000	**0.040**	0.000
4	3	0.069	0.071	0.057	0.000	0.000	**29.301**	0.000	0.009	0.013	0.005	0.000	0.005	0.000	0.000	0.006	0.000	0.000	0.000	0.002	**0.007**	0.000	0.000	0.012	0.000
4	4	0.000	0.000	0.000	**0.028**	0.000	**11.651**	**0.049**	**0.012**	**0.019**	0.000	0.000	0.000	0.002	0.002	0.004	0.004	0.000	0.006	0.004	**0.013**	0.000	0.000	**0.030**	0.007
5	1	0.069	0.057	0.026	**0.044**	0.000	**15.111**	0.000	**0.012**	**0.032**	0.000	0.000	0.000	0.000	0.006	0.006	0.000	0.000	0.000	0.001	**0.009**	0.000	0.000	0.019	0.000
5	2	**0.625**	**0.248**	0.034	**1.573**	0.000	**12.990**	0.000	**0.027**	**0.048**	0.000	0.000	0.006	0.000	0.013	0.000	**0.013**	**0.354**	0.000	0.000	**0.011**	0.000	0.000	0.015	0.000
5	3	0.211	0.121	**0.075**	**0.060**	0.000	**18.334**	0.000	**0.022**	**0.040**	0.004	0.000	**0.007**	0.007	0.008	0.000	0.000	0.007	0.003	**0.009**	**0.007**	0.000	0.002	0.025	0.000
5	4	0.263	0.161	0.061	**0.064**	0.000	**23.103**	0.000	0.008	0.003	0.000	0.000	0.000	0.000	0.000	0.000	0.001	**0.009**	0.000	0.001	0.005	0.000	0.002	0.000	0.000
6	1	0.000	0.000	0.053	**0.041**	0.000	**12.482**	0.000	0.001	**0.015**	0.000	0.000	0.001	0.000	0.000	0.000	0.000	0.000	0.000	0.000	0.000	0.008	0.002	**0.022**	0.000
6	2	0.291	**0.191**	0.046	**0.122**	0.000	**11.199**	0.000	0.003	**0.019**	0.005	0.000	0.002	0.000	0.000	0.000	0.000	0.000	0.000	**0.009**	**0.008**	0.011	0.000	0.003	0.000
6	3	0.086	0.080	0.068	**0.169**	0.000	**10.491**	0.000	0.000	**0.016**	0.001	0.000	**0.009**	0.003	**0.036**	**0.009**	0.003	0.001	0.000	0.006	0.003	0.006	0.000	0.000	0.000
Mean		0.323	0.091	0.050	0.175	0.000	19.605	0.029	0.010	0.031	0.003	0.000	0.003	0.001	0.011	0.002	0.002	0.018	0.000	0.004	0.010	0.005	0.001	0.013	0.001
SD		0.474	0.092	0.034	0.334	0.001	13.132	0.083	0.009	0.026	0.003	0.001	0.003	0.002	0.015	0.003	0.003	0.073	0.001	0.004	0.007	0.008	0.003	0.014	0.002
Min		0.000	0.000	0.000	0.000	0.000	0.024	0.000	0.000	0.000	0.000	0.000	0.000	0.000	0.000	0.000	0.000	0.000	0.000	0.000	0.000	0.000	0.000	0.000	0.000
Max		1.674	0.338	0.140	1.573	0.005	43.220	0.301	0.030	0.097	0.013	0.004	0.009	0.007	0.057	0.009	0.013	0.354	0.006	0.014	0.029	0.029	0.007	0.045	0.010

As shown in Table 2, $PM_{2.5}$ mass was variable across the different scenarios investigated, with values ranging from 2.3 $\mu g/m^3$ to 256 $\mu g/m^3$. The low value for the primary particle scenario is not surprising (Round 1), given the known high efficiency of the electrostatic precipitator at this plant.

In Rounds 2 and 3 (neutralized secondary particles + SOA), acidity was low and OC was high, as expected. The sum of sulfate and OC approximated the total $PM_{2.5}$ mass.

In Round 4 (unneutralized secondary particles + SOA), acidity was high, as expected, as was OC, whereas ammonium was very low. However, collection of particle phase OC on quartz fiber filters with subsequent thermal optical reflectance (TOR) measurement of EC and OC on the filters is only a semi-quantitative method. It is recognized that some vapor phase organic species (VOCs) are collected along with the particles, yielding an overestimate of particle phase OC. Early attempts to compensate for the collection of VOCs used a second filter downstream of the particle collection filter. It was assumed that only a relatively small fraction of the VOCs would be trapped on the first filter, and therefore almost the same amount of VOCs would be trapped on the second filter. Therefore, by subtracting the amount of OC on the second filter from the total OC on the first filter, a better estimate of particle-phase OC could be made. However, when tests were done using a diffusion denuder to remove VOCs upstream of the first filter, significant amounts of OC were found on the second filter. The explanation for this result was that there are some organic species that are semi-volatile, and can be partitioned between vapor and particle phase. When the denuder is used, the equilibrium distribution of particle and gas phase for the semi-volatile organics (SVOCs) is displaced, and the particle-phase SVOCs volatilize. Therefore, there is in fact no simple way to know from measurements using one or two filters, with and without a denuder, how much of the OC was in particle phase in the sampled air. For the samples in this study, we expect relatively high concentrations of both VOCs and SVOCs, so the true particle-phase OC concentration (as represented by a fraction of the total mass collected on a Teflon filter) is probably less than that measured as OC on the quartz filter. For atmospheric particle-phase OC, typically the OC (reported here as mass of carbon only) is multiplied by a factor, usually 1.4, to take into account the hydrogen and oxygen associated with the carbon. If this factor was applied to the OC (as carbon) reported in Table 2, then the sum of sulfate and OC mass concentrations would be greater than the gravimetrically measured mass concentration. But since we expect a significant fraction of the measured OC (as carbon) was due to VOCs, this mass concentration comparison can be interpreted as showing reasonable agreement.

During Round 5 (neutralized secondary particles + SOA), there were no qualitative or quantitative changes in the composition of PM compared with Rounds 2 and 3 conducted in June/July. Acidity was low and OC was high, and the sum of sulfate and OC approximated the total $PM_{2.5}$ mass. OC was not as high as for the earlier run in October. There was also an unexplained decrease in the total secondary aerosol and sulfate generated, and an increase in nitrate.

During Round 6 (unneutralized secondary particles), PM mass was also lower than expected. It is unclear why OC is elevated in this scenario without secondary organic aerosol. It may be that VOCs or SVOCs adsorbed onto chamber walls and other surfaces in the earlier tests volatilized subsequently and were collected on the quartz filters. Again, as with Round 5, sulfate was lower than expected.

The very low values of measured elemental carbon that were observed are not likely to have originated in the stack gas (given that the overall dilution from stack to exposure chamber is 1500-2000 times) and we were also informed by the plant operators that with the extra capacity

ESPs used, no measurable EC is emitted. However, although ESPs do remove EC-containing particles, they do so with less efficiency than for non-conductive particles, so some EC particles do penetrate. Also, the plant operator's method of measuring EC is much less sensitive than the TOR method. Moreover, none of the chemical reactions are expected to produce EC. However, the measured OC values are quite a bit higher than the EC values. It is quite reasonable to assume that the EC values result from the uncertainty in the thermal optical reflectance method. As the OC is heated, some of it forms a char containing elemental carbon. The method is supposed to correct for this by measuring the change in optical reflectance. If the change in optical reflectance due to charring underestimates the amount of OC that charred, then the remaining char will give a positive artifact EC value.

Concentrations of pollutant gases were low in all six experimental runs (Table 3). This is important given the effects of ozone, NO_2, and SO_2 on respiratory endpoints.

Table 4 shows the elemental results for the different scenarios investigated. The results are bold for those values that are at least twice the uncertainty values. Because there may be some usefulness for values less than twice the uncertainty, they are also included in the table. Note also that each sample has a different set of uncertainty values because with XRF, the uncertainty is related to corrections for interference by elements with higher atomic number than any given element, and the distribution of element magnitudes is different for each sample.

All elements were present at low concentrations, with the exception of sulfur, which was present in oxidized emissions samples at 10 – 43 $\mu g/m^3$. Silicon, calcium, and bromine were commonly detected in multiple samples. Less commonly observed elements included Mg, Al, Cl, K, Cr, Fe, Ni, Cu, Zn, Se, Ba, and Hg.

Differences in metal concentrations between scenarios may be a result of variations in stack emission mass concentrations reflecting differences in the size distribution of particles. The operation of the electrostatic precipitator may be sufficiently variable to allow such differences. We were informed by the plant operators that the same coal was used for the entire duration of the tests, but this only means that the coal came from the same source. However, it is possible that even for the same source there was enough variation in coal composition to account for the observed differences.

3.3 Toxicological Results

The toxicological results for all experiments are presented below. In the case of the most complex scenario, which was carried out in triplicate, all animals were combined. The total number of animals for each scenario is shown in Table 5.

Table 5. Number of experimental animals per scenario.

	Respiratory Parameters		BAL Parameters		Blood Parameters	
Scenario	Control	Exposed	Control	Exposed	Control	Exposed
Primary	20	20	0	0	12	12
Secondary	15	15	5	5	9	9
Secondary + SOA	60	60	18	18	36	36
Secondary + NH_3 + SOA	20	20	6	6	12	12

Pulmonary Function and Breathing Pattern

No differences between exposed and control animals were observed for any of the pulmonary function/breathing pattern parameters examined. Figures 7 and 8 show example results for respiratory frequency and Enhanced Pause, respectively.

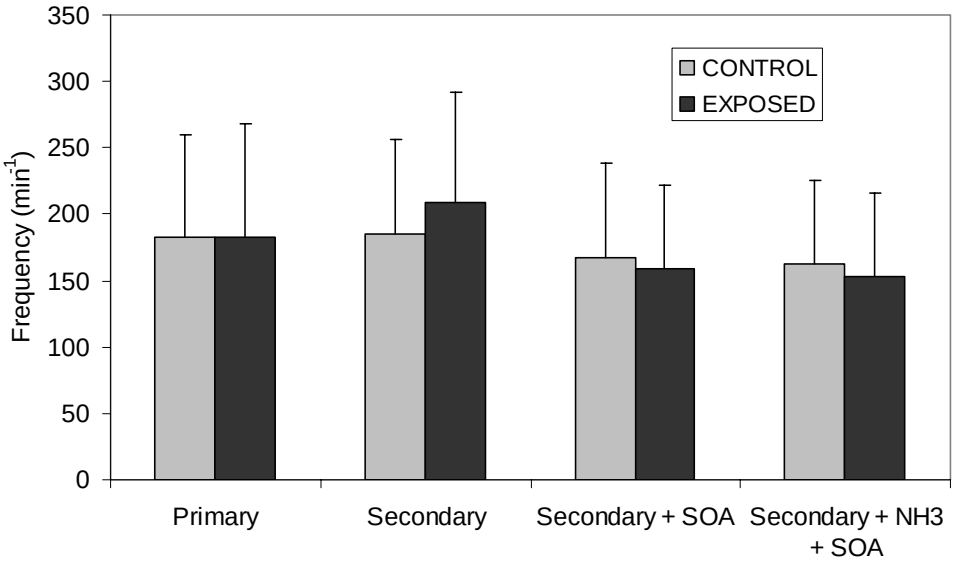

Figure 7. Respiratory frequency in Sprague-Dawley rats exposed to different power plant emission scenarios, May-November, 2004.

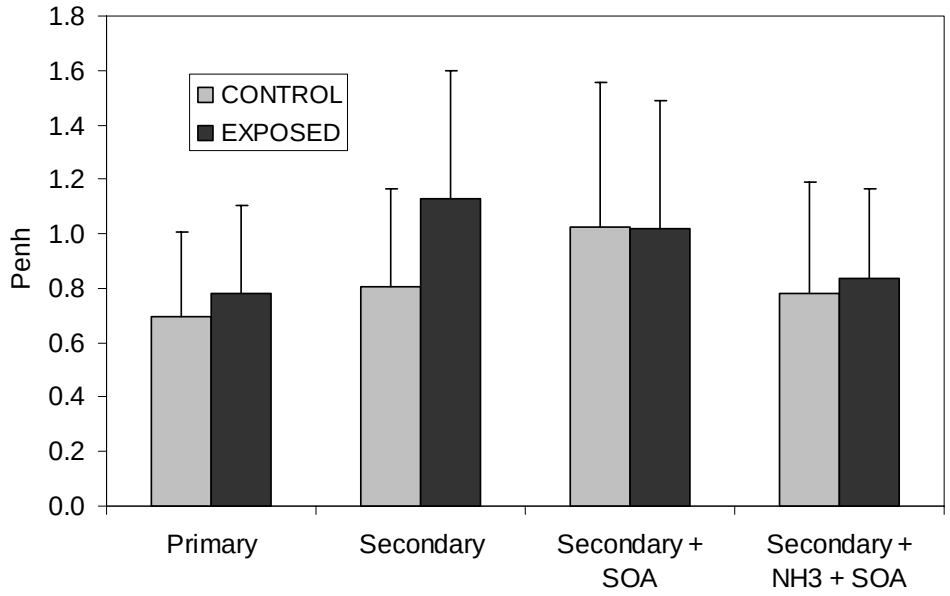

Figure 8. Enhanced Pause (Penh) as a measure of bronchoconstriction in Sprague-Dawley rats exposed to different power plant emission scenarios, May-November, 2004.

Bronchoalveolar Lavage

Selected results of the BAL fluid analyses are shown in Figures 9 and 10. No significant differences between exposed and control animals were observed for cytological parameters (total cell count, neutrophils, macrophages, lymphocytes, eosinophils, epithelial cells) or biochemical markers (LDH, βNAG, and total protein).

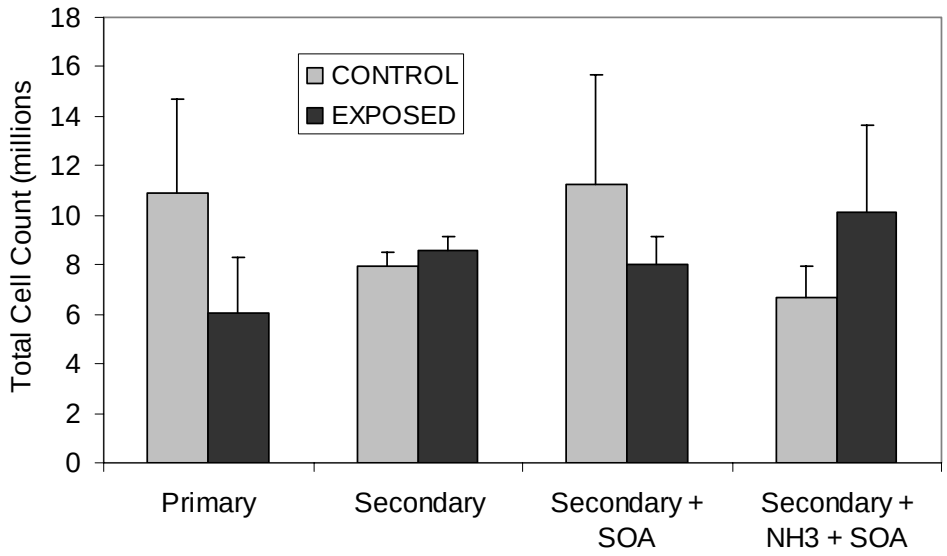

Figure 9. Total cell count in BAL fluid from Sprague Dawley rats after exposure to different power plant emission scenarios, May-November, 2004.

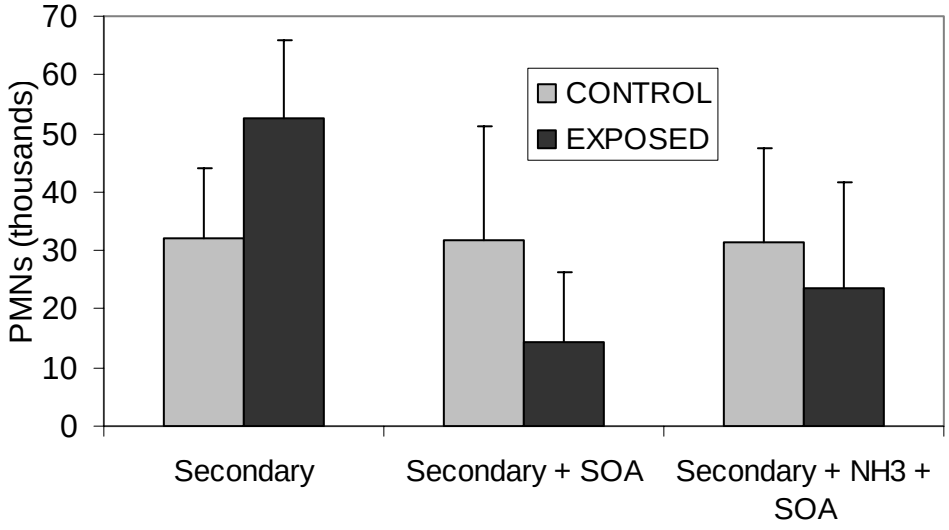

Figure 10. Polymorphonuclear neutrophils (PMNs) in BAL fluid from Sprague Dawley rats after exposure to different power plant emission scenarios, May-November, 2004.

Blood Cytology

Results of selected blood cytological analyses are provided in Figures 11 and 12 below. No significant differences between exposed and sham animals were observed for Hgb & Hcrt, pllatelet count, white blood cell count, neutrophils, lymphocytes, monocytes, or eosinophils.

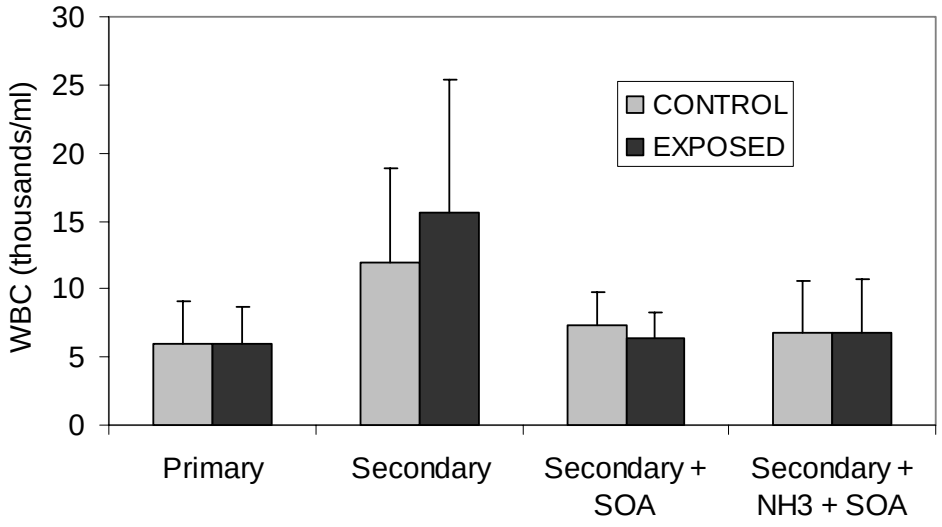

Figure 11. White blood cell counts, Sprague-Dawley rats after exposure to different power plant emission scenarios, May-November, 2004.

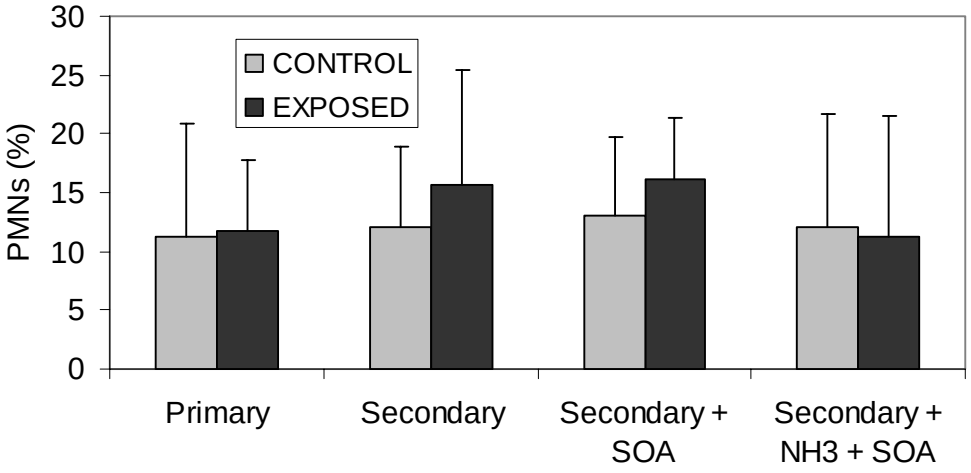

Figure 12. Blood polymorphonuclear neutrophils in blood from Sprague-Dawley rats after exposure to different power plant emission scenarios, May-/November, 2004.

In Vivo Oxidative Stress

Oxidative stress was determined using in vivo chemiluminescence of heart and lung tissue. In addition, to confirm the chemiluminescence findings, the TBARS (thiobarbituric acid reactive substances) assay was carried out for the two scenarios completed in October. Only TBARS was employed in the November sampling round. Results are shown in Figures 13-15.

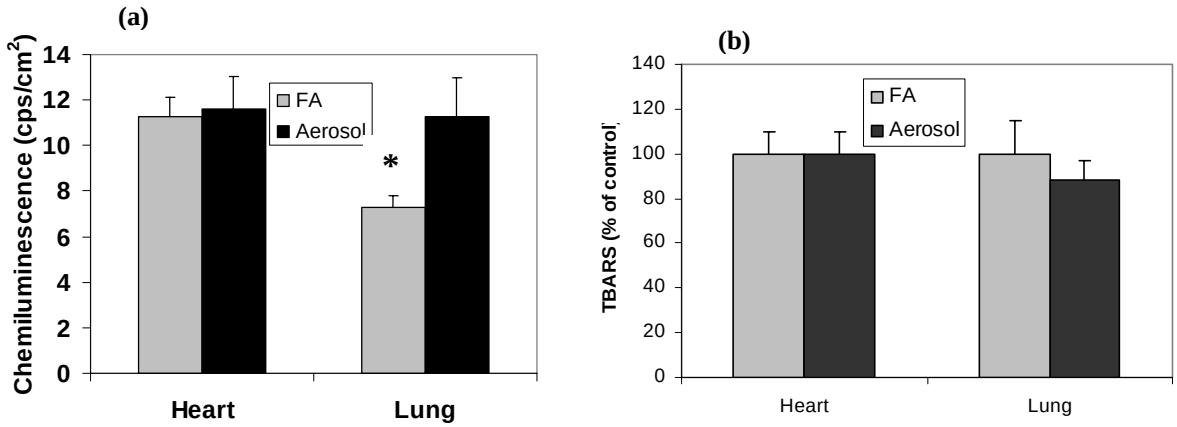

Figure 13. Oxidative stress in Sprague-Dawley rats exposed to oxidized, neutralized emissions and secondary organic aerosol. (a) Chemiluminesence, pooled animals, June and October, 2004. *n*= 22 for control, heart; 21 for exposed, heart; 19 for control, lung; and 17 for exposed, lung. (b) TBARS, October, 2004. *n*=8 for all groups. * indicates significant difference between sham and exposed animals ($p<0.05$) using a 2-tailed t-test.

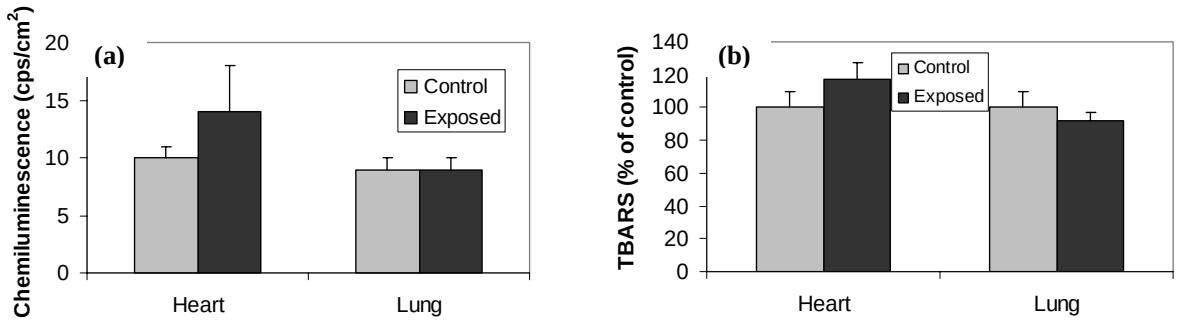

Figure 14. Oxidative stress in Sprague-Dawley rats exposed to oxidized emissions and secondary organic aerosol, October 4-7, 2004. (a) Chemiluminesence, *n*= 6 for control, heart; 7 for exposed, heart; 7 for control, lung; and 8 for exposed, lung. (b) TBARS, *n*=8 for all groups.

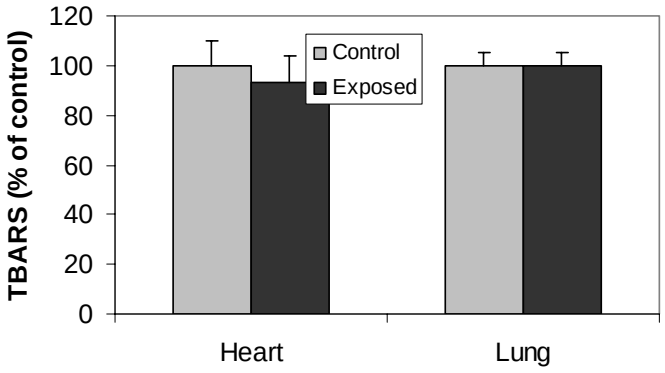

Figure 15. TBARS results for Sprague-Dawley rats exposed to oxidized emissions, November 3-5, 2004. *n*= 8 for all groups.

For the combined (pooled) June and October exposures to the most complex scenario (oxidized, neutralized + SOA), a difference in the chemiluminescence lung response was observed in the exposed group (Figure 13). However, although the difference was statistically significant, this difference was primarily driven by the lower chemiluminescence values observed in control animals during the October exposures. When compared with the pooled data for all the control animals, or with the data for control animals exposed to this scenario in June, the aerosol exposed group showed no significant increase in chemiluminesence.

No significant differences between exposed and sham animals were observed following exposure to secondary + SOA or secondary alone scenarios (Figures 14 and 15, respectively).

Histopathology

Histopathological analyses to assess evidence of inflammation in lung airways and parenchyma, and vasoconstriction in lung and cardiac blood vessels, were carried out. Results showed no evidence of such effects.

4.0 MOBILE SOURCE EMISSIONS TESTING

The project also includes assessment of the toxicity of mobile source emissions, being funded from other sources. However, these experiments have not yet been conducted due to the mobile laboratories being occupied with the coal combustion emissions work. The mobile source work will be conducted at the conclusion of the TERESA program, after the three plants have been investigated, and the findings will be reported in an addendum to this report.

5.0 CONCLUSIONS AND FUTURE DIRECTIONS

We investigated four exposure scenarios at a power plant in Wisconsin burning Powder River Basin coal, and no adverse biological effects were observed. Results indicated no differences between exposed and control animals in any of the endpoints examined. Exposure concentrations for the scenarios utilizing secondary particles (oxidized emissions) ranged from 70 - 256 $\mu g/m^3$, and some of the atmospheres contained high acidity levels (up to 49 $\mu g/m^3$ of equivalent

unneutralized H_2SO_4). However, caution must be used in generalizing these results to other power plants utilizing different coal types and with different plant configurations, as the emissions may vary based on these factors.

This project is part of a larger research effort, the TERESA (Toxicological Evaluation of Realistic Emissions of Source Aerosols) Study. TERESA includes fieldwork and assessment of health effects at three power plants: (1) the subject plant in this report, located in Wisconsin; (2) a plant in the Southeast burning low-to-medium eastern bituminous coal; and (3) a plant in the Midwest burning medium-to-high eastern bituminous coal, with a scrubber. Work at these latter two plants is being partially funded by the U.S. Department of Energy's National Energy Technology Laboratory (DOE-NETL). For additional information on this larger study, please visit http://www.netl.doe.gov/coal/E&WR/air_q/index.html.

7.0 REFERENCES

Alarie, Y.M., Krumm, A.A., Busey, W.M., et al. 1975. *Arch. Env. Health* 30:254-262.

Barnard, ML, Gurdian, S, and Turrens, JF 1993. *J Appl Physiol* 75:933-939.

Boveris, A., Cadenas, E., Reiter, R., Filipkowski, M., Nakase, Y., and Chance, B. 1980. Organ chemiluminescence: noninvasive assay for oxidative radical reactions. *Proc. Nat. Acad. Sci.* 77:347-351.

Boveris, A and Cadenas, E. 1999. Reactive oxygen species in biological systems. An interdisciplinary approach, Gilbert, DL and Colton, CA, Eds. Plenum Publishers, New York, NY.

Evelson, P., and González-Flecha, B. 2000. Time course and quantitative analysis of the adaptive responses to mild hyperoxia in the rat lung and heart. *Biochim. Biophys. Acta* 1523:209-216.

Gurgueira, SA, Lawrence, J, Coull, B, et al. 2002. *Environ. Health Perspect,* 110: 749-755.

Holmes, M. 2002. An outdoor multiple wavelength system for the irradiation of biological samples: analysis of the long-term performance of various lamp and filter combinations. *Photochem. Photobiol.* 76 (2):158-163.

Klemm, R.J.; Lipfert, F.W.; Wyzga, R.E.; Gust, C. 2004. Daily mortality and air pollution in Atlanta: two years of data from ARIES. *Inhal. Toxicol.* 16 (Suppl 1):131-141.

MacFarland, H.N., Eulrish, C.E., Martin, A., et al. Inhaled Particles III, ed. W.H. Walton, pp. 313-326, Unwin Brothers Ltd., Surrey.

McLeod, A. 1997. Outdoor supplementation systems for studies of the effects of increased Uv-B radiation. *Plant Ecology* 128 (1-2):78-92.

Metzger, KB. Tolbert, PE, Klein, M, Peel, JL, Flanders, WD, Todd, K, Mulholland, JA, Ryan, PB, Frumkin, H. 2004. Ambient air pollution and cardiovascular emergency department visits. *Epidemiology,* 15(1):46-56.

Pesce, A., McKay, R.H., and Stolzenbach, F. 1964. The comparative enzymology of lactic dehydrogenase. I. Properties of the crystalline beef and chicken enzymes. *J. Biol. Chem.* 239:1753-1761.

Peel, JL, Tolbert, PE, Klein, M, Metzger, K, Flanders, WD, Todd, K, Mulholland, J, Ryan, PB, Frumkin, H. 2005. Ambient air pollution and respiratory emergency department visits. *Epidemiology* 16(2):155-163.

Raabe, O.G., Tyler, W.S., Last, J.A., et al. 1982. *Ann. Occ. Hygiene* 26:189-211.

Ruiz, P.A., Gupta, T., Kang, C-M., Lawrence, J.E., Ferguson, S.T., Wolfson, J.M., Rohr, A.C., and Koutrakis, P. 2005a. Development of a system for the toxicological evaluation of particles generated from coal-fired power plants. Manuscript in preparation.

Ruiz, P.A. Lawrence, J.E., Wolfson, J.M., Ferguson, S.T., Gupta, T., Kang, C-M., and Koutrakis, P. 2005b. Development and evaluation of a photochemical chamber for the toxicological study of coal combustion emissions. Manuscript in preparation.

Ruiz, P.A., Lawrence, J.E., Ferguson, S.T., Wolfson, J.M., and Koutrakis, P. 2005c. Development and laboratory evaluation of a counter-current parallel plate membrane denuder for the nonspecific removal of gases from an aerosol stream. *Environ. Sci. Tech.*, submitted.

Schreider, Y.P., Culbertson, M.R., and Raabe, O.G. 1985. *Environ. Res.* 38:256-274.

Sellinger, O.Z., Beaufay, H., Jacques, P., Doyan, A., and Deduve, C. 1960. Tissue fractionation studies, intracellular distribution and properties of β-n-acetyl-glucosaminidase and β-galactosidase in rat liver. *Biochem. J.* 74:450-456.

Sinclair, A.H. and Tolsma, D. 2005. Associations and lags between air pollution and acute respiratory visits in an ambulatory care setting: 25-month results from the Aerosol Research and Inhalation Epidemiology Study (ARIES). *J. Air Waste Manage. Assoc*. 54:1212-1219.

Turrens, JF, Giulivi, C, Pinus, CR, et al. 1988. *Free Rad Biol Med* 5:319-323.